Optimized synthesis/design of the carbonator side for direct integration of thermochemical energy storage in small size Concentrated Solar Power

Energy Conversion and Management: X 4 (2019) 100025

Contents lists available at ScienceDirect

Energy Conversion and Management: X

journal homepage: www.journals.elsevier.com/energy-conversion-and-management-x

Optimized synthesis/design of the carbonator side for direct integration of thermochemical energy storage in small size Concentrated Solar Power

U. Tesio[a,*], E. Guelpa[a], C. Ortiz[b], R. Chacartegui[c], V. Verda[a]

[a] Energy Department, Politecnico di Torino, Turin, Italy
[b] Facultad de Física, Universidad de Sevilla, Avenida Reina Mercedes s/n, 41012 Sevilla, Spain
[c] Escuela Técnica Superior de Ingeniería, Universidad de Sevilla, Camino de los descubrimientos s/n, 41092 Sevilla, Spain

ARTICLE INFO

Keywords:
Concentrated Solar Power
Calcium-Looping
HEATSEP
Brayton cycle
Long term energy storage

ABSTRACT

Two of the most attractive characteristics of Concentrated Solar Power are the high-quality heat exploitable and its capacity for thermal energy storage, which enhance the energy dispatchability in comparison with other renewable sources such as photovoltaics or wind. Consistent efforts are therefore direct to the research of suitable thermodynamic cycles and energy storage systems with low thermal losses and high operating temperatures. However, in the most developed technologies, based on sensible and latent heat storage, high thermal losses are the direct consequence of high operating temperatures. As alternative, Thermochemical Energy Storage systems are gaining attention in the last years.

The present work investigates the adoption of a novel Calcium-Looping system for Thermochemical Energy Storage, focusing on the integration on carbonator side. This key integration is directly linked to the energy delivery from the energy storage system and therefore power generation capacity of the plant. An optimization of the carbonator side plant is performed for a direct integration layout, where carbon dioxide from the carbonator evolves through the power block. This analysis aims to maximize the system efficiency acting both on the process components operation and on the thermal transfer between the involved streams. The optimization relies on a novel method based on a genetic algorithm. The pinch analysis is adopted for this study and proper constraints are provided to obtain a configuration exploiting only the renewable energy source. A multi-objective optimization is performed to find out the heat exchanger network topology changes that occur for different operating conditions and derived from this analysis suggestion for systems integration are provided.

1. Introduction

The number of Concentrated Solar Power (CSP) plants under-development [1], the total capacity forecasts for the next few years and the expected falling costs (with a consequent Levelized Cost Of Electricity decrease) [2] show the great interest and potential of Concentrated Solar Power plants. The possibility to exploit high temperatures and, therefore, the availability of high-quality heat, is one of the characteristics of this technology. Dispatchability in renewable energy plants is a major issue to be improve in next years to overcome the inherent intermittency of the sources [3]. Moreover, thermal energy storage is fundamental to maintain a constant electrical production, to avoid a plant oversizing and to keep the operating conditions as close as possible to the nominal configuration. Among the different energy storage technologies in CSP plants [4], Thermochemical Energy Storage (TCES) based on Calcium Looping, is one of the most promising alternatives [5,6] due to a high energy storage density and a potentially higher maximum temperature in the power cycle because of the high reactions temperature [7]. Other consistent advantages related to Calcium-Looping (CaL) TCES are: i) a low cost material involved by the process (< 10 €/ton [8]); ii) reduced cost of the TCES itself as it is based on well-known equipment at industrial scale (excepting the solar particle receiver) [9]; iii) negligible thermal losses during the storage period (vessels are kept at ambient temperature) and therefore the possibility of long term energy storage [10]. All these considerations contributed to start up the European project SOCRATCES [11], whose aim is to demonstrate (both theoretically and on a prototype scale) the feasibility of a Calcium-Looping integration in a CSP plant.

Suitable power blocks for the energy production in the CSP field are proposed in [12–14]; the most common alternatives are Rankine cycles, integrated with molten salts storage, and CO_2 Brayton cycles, with heating directly performed at the receiver. In this work a specific

* Corresponding author.
E-mail address: umberto.tesio@polito.it (U. Tesio).

https://doi.org/10.1016/j.ecmx.2019.100025
Received 26 July 2019; Received in revised form 12 October 2019; Accepted 14 October 2019
Available online 21 October 2019

Nomenclature

$CaCO_3$	Calcium carbonate
CaO	Calcium oxide
CO_2	Carbon dioxide
EI	Excess index
h	Specific enthalpy, kJ/kg
$\dot{m}$	Mass flowrate, kg/s
M	Mixer
MC	Main compressor
MT	Main turbine
n	Number of moles
P	Pressure, bar
ST	Storage turbine
T	Temperature, K
U	Global heat transfer coefficient, kW/(m^2*K)
X	CaO conversion
$\dot{W}$	Power flux, kW

Abbreviations

CaL	Calcium-Looping
CCS	Carbon Capture and Storage
CIP	Compressor inlet pressure, bar
CIT	Compressor inlet temperature, K
COP	Compressor outlet pressure, bar
COT	Compressor outlet temperature, K
CSP	Concentrated Solar Power
HEN	Heat Exchangers Network
HEX	Heat exchanger
LCOE	Levelized Cost Of Electricity
ORC	Organic Rankine Cycle
TIP	Turbine inlet pressure, bar
TIT	Turbine inlet temperature, K
TOP	Turbine outlet pressure, bar
TOT	Turbine outlet temperature, K

Greek letters

Δ	Delta
β	Pressure ratio
η	Carbonator side efficiency
φ	Thermal flux, kW

Subscripts and superscripts

0	standard conditions
amb	ambient
carb	carbonator
stoic	el
in	inlet
lm	logarithmic mean
mix	mixed
out	outlet
pp	pinch point
r	reaction
rec	recirculated
stoic	stoichiometric
stor	storage
un	unreacted

analysis for the integration of the CaL process is performed focused on the integration of the carbonator, the reactor where the storage energy is release to the power cycle. Fig. 1 shows a conceptual scheme of the CSP-CaL integration; very briefly, the stored $CaCO_3$ is preheated and sent to the calciner, where, absorbing the solar radiation (φ_{sol}), is converted into CaO and CO_2, which are cooled down and sent to their storages. Being stored at high pressure, the CO_2 is compressed and again cooled. For the discharge phase it is heated up, expanded and mixed with a recirculated stream; then, both the CaO and the CO_2 are preheated and enter the carbonator. The solid stream exiting the reactor is brought to the storage conditions, while the gaseous flow is expanded, cooled down and compressed in order to be recirculated.

There are two different ways to design the carbonator-power cycle integration: i) by using the CO_2 stream exiting the carbonator as working fluid for power production or ii) through an indirect integration based on a separate thermodynamic cycle fed by a thermal recovery performed on the carbonation products. A deep investigation about the former alternative is conducted in [15], the expansion of the CO_2 extracted from the storage is thermally coupled with the compression of the CO_2 recirculated from the carbonator in order to maximize the expansion work and minimize the compression absorption respectively. In [16] is proposed a direct CaL integration with an air/CO_2 open cycle showing high performances and a simple layout but whose operation determines the release to the atmosphere of an effluent gas not CO_2-free; the importance of the heat recovery both for the charging and discharging phase of this configuration is demonstrated in [17]. A detailed study performed in [18] compares the performances of both direct integration with closed CO2 cycle and the indirect integration of some suitable power blocks (Rankine cycle, SCO2 Brayton cycle and combined cycle). An alternative CaL layout is investigated in [19], where the energy storage occurs at high temperature to simplify the process integration scheme. Similar to this last configuration, but with a more complex design, in [20] is analyzed the choice of a direct (closed CO_2 loop) or indirect (Rankine cycle) integration in series with an Organic Rankine Cycle (ORC) for the low-temperature heat recovery. Furthermore, a study for the adoption of a CaL direct integration for the storage of energy produced by photovoltaic (PV) is performed in [21], demonstrating a significantly lower plant investment

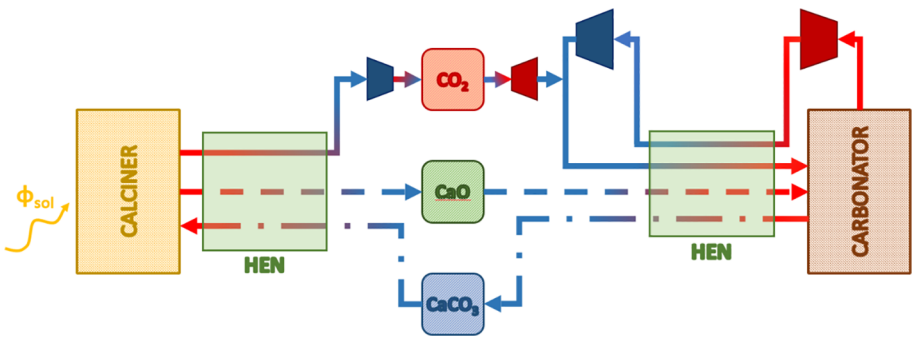

Fig. 1. CaL direct integration essential schematic.

cost when compared to batteries. Most of these works are summed up in [8], where the different layouts are compared both in terms of efficiency and characteristics.

However, in the analysis performed in these works are present some drawbacks: in some cases the CaL integration is not optimized, the CO_2 compression/expansion stages become particularly complex (up to 8 intercoolings/reheatings), the use of heaters does not allow to operate with a completely renewable energy source or a poor number of variables is assumed in the optimization process. The aim of this work is to investigate the promising application of the CaL direct integration in a central tower CSP plant based on an innovative method which applies the pinch analysis [22] for the synthesis of an optimized design in which the mentioned issues are solved. In this novel methodology, plant efficiency maximization is attained through the simultaneous optimization of both the heat exchange and components performance. Main novelties and contributions of this paper are: 1) a full optimization framework, the HEATSEP [23] (described in Section 3), which is applied for the first time to the synthesis/design of the discharge section of the CaL-CSP plant, allowing to perform an optimization of all the independent variables of the process; 2) unlike the traditional investigations performed with the HEATSEP method, where the analysis ends with the calculation of the thermal integration curves and the Heat Exchanger Network (HEN) remains therefore unknown, in the present work the HEN is designed for the optimized configuration and the considerations made for this layout are exploited in the run of a second optimization, providing a further improved design; 3) a multi-objective optimization is performed in order to investigate the possible trade-off between the plant performances and its heat recovery system complexity and size, proposing a novel approach to the traditional HEATSEP method, in which the HEN stiffness is not taken into account; and 4) a 100% renewable external heating requirement is imposed in the analysis thus obtaining configurations which fully exploit the solar resource.

The paper is structured as follows:

- Section 2: the most important aspects and characteristics related to the CaL direct integration are discussed;
- Section 3: the plant simulation and optimization are explained;
- Section 4: the energy optimization results are reported and commented;
- Section 5: the multi-objective optimization is performed in;
- Section 6: some suggestions for the plant layout improvement are provided;
- Section 7: some considerations with a more general extent are exposed;
- Section 8: paragraph dedicated to the analysis conclusions.

2. Case study

As presented in [18], the direct integration is one of the most interesting alternatives for CSP power production between the CaL integration alternatives: it shows an excellent performance, the best between the other investigated cycles, and its layout is relatively simple if compared to the indirect integrations, involving a reduced number of components, most of them well-known at industrial scale. In the calciner side, after a preheating process, the solid stream made of both $CaCO_3$ and unreacted CaO enters the calciner reactor. Under pure CO_2 atmosphere, calcination temperature has to be around ~930–950 °C to ensure complete calcination in short residence times [24]. Lower calcination temperatures are needed by performing the calcination under He or steam [25–27], although in this case the energy penalty could be higher due the separation process energy consumption. After calcination, CO_2 and CaO are cooled down and sent to their storage vessels. To manage the storage tanks size, CO_2 is compressed up to its design pressure of 75 bar [18,19] and [28] and, in order to minimize the compression work required, one or more intercooling steps should be included. Anyway, as explained further on, the carbon dioxide will be re-expanded and part of the energy previously consumed is recovered, reducing considerably the energetic penalty brought by its compression [15]. Due the storage step, the calciner and carbonator sides work independently and therefore the layout can be optimized separately.

In the CaL discharge process, CO_2 is extracted from the storage tank, heated and expanded up to the carbonator operating pressure. Even in this case, in order to maximize the expansion work, can be added one or more reheating steps. The other reactant, the CaO, is preheated and sent to the reactor to produce calcium carbonate according the exothermal carbonation reaction. After carbonation, solids are separated from the gaseous stream and the CO_2 is expanded in the main turbine; then, sensible heat is recovered from both CO_2 and solids steams. Finally, the carbon dioxide is compressed and recirculated inside the process, while the $CaCO_3$ and the unreacted CaO are sent to storage vessels.

Both in the calciner and carbonator side is required to move the solid streams at high temperature entering or exiting the chemical reactors. This can be done by screw conveyors as proposed by [28] and demonstrated in practice by the Carina European Project [29] and [30]; furthermore, the same technology but with a vertical configuration can be exploited as solid elevator [31].

Two of the main parameters that have a particular influence on the entire CaL process are the CaO conversion (X) and the CO_2 excess index (EI). CaO conversion (also referred as CaO activity or reactivity) is defined as the mass ratio between the calcium oxide that participates actively to the carbonation reaction and the total amount entering the reactor; this term is defined because, in real operation conditions, CaL process is not completely reversible [32]. After a few cycles, multicyclic CaO deactivation decays up to reach a residual value, which is highly dependent on the reactor conditions, the particle size and the CaO precursors used [8]. CO_2 excess index expresses the surplus of carbon dioxide that is sent to the carbonator in order to control the operating temperature. It is defined as the ratio between the total amount of CO_2 provided to the stoichiometric value.

$$X = \frac{n_{CaOreacted}}{n_{CaOprovided}} \tag{1}$$

$$EI = \frac{\dot{m}_{CO_2provided}}{\dot{m}_{CO_2stoich}} \tag{2}$$

For the purposes of this work, a small/medium size plant is analyzed, so, the net power output in correspondence of the main shaft (main turbine, main compressor and generator) is set to 1MWe. Therefore, with this power plant size, a reduced complexity layout is considered, with differences from some works found in literature for larger plants [18,33], where multiple stages of intercooling and reheating for respectively the main compressor and the storage turbine are suggested. In the present work, the processes of compression and expansion are performed in a single step, allowing to obtain a more essential layout. The minimum achievable pressure at the main turbine outlet is set to 1 bar; in fact, according to [15] and [19], avoiding operation under vacuum conditions leads the plant to operate under no particularly demanding conditions and both the pipelines and turbomachinery dimensions are not excessively penalized. This assumption brings to another benefit, since any eventual air infiltration (due to non-ideal sealings) is consequently eliminated.

The objective function assumed for the optimization process is the carbonator side efficiency, which is defined as follows

$$\eta_{carb} = \frac{\dot{W}_{net,el}}{\dot{Q}_{carb}} = \frac{\dot{W}_{net,el}}{\dot{m}_{CaO} \cdot X \cdot \Delta h_r^0} \tag{3}$$

where $\dot{m}_{CaO}$ is the CaO mass flow rate entering the carbonator, X is the CaO conversion and the net electric power production ($\dot{W}_{net,el}$) includes the contribution of main turbine, main compressor, storage turbine and auxiliaries (for heat rejection and solid conveying). This analysis does not include other aspects related to the complete CaL integration such

as the calciner side efficiency and the electricity consumed for the compression of the carbon dioxide up to the storage conditions. So, being referred to only a plant portion, for the aims of this study the carbonator side efficiency is sufficient to perform a coherent comparison for the TCES discharge process, differently from [15,18] and [33], where the entire process is simulated and the efficiency must be therefore defined differently.

The choice of the optimization structure is made in accordance with the objective of obtaining a configuration with the highest achievable efficiency for the case in which the solar radiation is the only external heat source. In order to optimize the plant operating conditions is required a layout composed by process components (turbines, compressors and chemical reactors) and by a suitable heat recovery system for the reactants preheating and the cooling required to reach the storage conditions. To ensure the optimum carbonator side configuration is not possible just analysing a specific HEN from a pinch analysis but also adopting an optimization stage able to maximize simultaneously the process operation and the heat exchangers network.

3. Model description/methodology

According to the optimization criteria previously exposed, the methodology that seems to be the most suitable for the present work is the HEATSEP method, which is exhaustively explained and applied to energy problems (power cycles, combined heat and power, industrial processes, heat recovery, etc.) in [34–36]. Very briefly, this method tackles separately the thermal power exchange and the other processes in which the plant streams are involved; this is made possible with the (virtual) substitution of all the heat exchangers with a single “black box” in which any fluid is free to transfer thermal power with the other ones. The simulation of this fictitious element is based on the pinch analysis. In this way it is possible to perform the energy plant optimization without providing a specific HEN for the entire execution of the process and leaving the heat exchangers definition to the postprocessing phase.

Therefore, after the substitution of any component involved in the heat exchange with a corresponding “thermal cut”, a configuration only constituted by process components and the black box is obtained, as showed in Fig. 2 (where MT is the Main Turbine, ST is the Storage Turbine, MC is the Main Compressor and M is the Mixer); the operation of this layout is optimized keeping the HEN undefined up to the last stage.

This initial step requires to take a first decision: in correspondence of the streams entering and exiting the mixer, the thermal cuts insertion can be executed in three different ways (shown in Fig. 3, where the dashed lines represents the insertion of a thermal cut and therefore a heat exchange step). The first alternative contains the smaller number of thermal cuts and therefore introduces the smaller number of heat exchange processes, in accordance with the purposes of simplifying as much as possible the plant layout.

Furthermore, in addition to the type of analysis executed in the works found in literature about the HEATSEP, an attempt to synthesize the optimum HEN is performed in the present paper.

All the data assumptions for the components and the involved processes are summed up in Table 1; in addition, the mixed streams of CO_2 are imposed to have the same pressure and both the mixer and the separator pressure losses are neglected. The values of these parameters are established in accordance to [18,19] and [37].

Regarding the thermophysical properties, the correlations in [38], the SysCAD database [37] and the COOLPROP library [39]are used for CaO, $CaCO_3$ and CO_2 respectively. Concerning the components simulation, turbomachinery performance is calculated through the isentropic efficiency, while the chemical reactor is simulated with energy balances adopted in [18] and [37], in which the fraction of calcium oxide that reacts with the carbon dioxide is imposed. The study performed is therefore 0-D (zero-dimensional, i.e. component’s geometry is not investigated) and the reactor type is not defined since the analysis of the reaction kinetics is not one of the purposes of the present work.

The successive step establishes how the different plant parameters (pressures, temperatures and flowrates) have to be handled within the optimization process, so, for first the storage physical conditions are assumed as constant. Then, after a careful evaluation of all the parameters involved in the analyzed process, a selection to establish the optimization terms is made (i.e. the independent variables of the problem) in order to obtain the maximum plant efficiency. They are: CaO activity (X), carbonator temperature (T_{carb}), carbonator pressure (P_{carb}), main turbine pressure ratio (β_{MT}), CO_2 temperature at the carbonator inlet ($T_{CO2,in}$), CaO temperature at the carbonator inlet ($T_{CaO,in}$), main compressor inlet temperature (CIT_{MC}) and storage turbine inlet temperature (TIT_{ST}). Furthermore, some of these layout parameters must satisfy design, thermal or technical constraints, such as the plant rated power, the absence of an external heating need and the minimum temperature achievable with the external cooling (see Table 2). At this point, starting from these constant terms, independent variables and constraints, any other physical quantity can be calculated performing the components simulation.

The variation ranges (reported in Table 3) provided to the independent variables have to be both physically and technically feasible, so they are again set in accordance to [18,19] and [37]. Regarding the carbonator operating temperature and pressure, it is verified that the values assumed (marked in green in Fig. 4) are respectful of the limitations determined by the equilibrium conditions.

Once the process components simulation is completed and all the pressures, temperatures and flowrates are calculated, it is possible to execute the pinch analysis on the streams that go across the black box. These flows involved in heat transfer and their relative data are reported in Table 4. The fifth stream, although listed between the cold fluids, is actually free to become a hot or cold flow, since no constraints are specified about that. This is established in order to avoid any limitation on the parameters space in which the optimal configuration is analyzed.

Taking into account the variables number, the problem constraints and the expected fitness function complexity, the genetic algorithm is chosen as optimization method and its execution is performed on MATLAB software. Fig. 5 shows with a flow chart the structure of the complete optimization process, which can be synthetically described as a pinch analysis nested in the evolutionary algorithm. The difference between the method used in the present work and the simple pinch

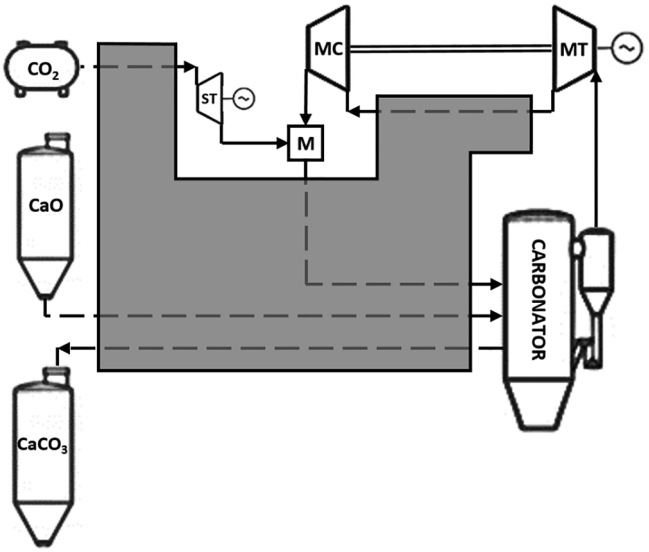

Fig. 2. Carbonator side layout for the optimization based on the HEATSEP method.

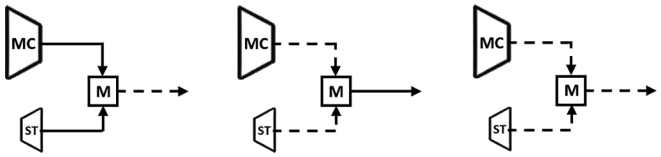

Fig. 3. Thermal cuts insertion alternatives in correspondence of the mixer.

Table 1
Data assumption for the main parameters involved in the process.

Parameter	Component/stream	Value
Thermal losses	Carbonator	1% of reaction heat
Storage temperature (T_{AMB})	CaO, CO_2, $CaCO_3$	20 °C
Storage pressure	CO_2 storage	75 bar
Pressure losses	Stoichiometric CO_2	1%
	Recirculated CO_2	4%
	Mixed CO_2	6%
Isentropic efficiency	MT	0.9
	MC	0.87
	ST	0.75
Mechanical and electrical efficiency	(MT + MC), ST	0.97
Solid conveying electrical consumption	CaO, $CaCO_3$ streams	10 kJ/(kg*100 m)
Storages-carbonator distance	CaO, $CaCO_3$ streams	100 m
Heat rejection electrical consumption	Coolers	0.8% of heat rejected
Minimum ΔT at pinch point	Heat exchangers	15 °C

Table 2
Optimization problem's constraints.

Parameter	Component/stream	Value
Net power production	MT + MC	1 MW
External heating need	Heaters	0 MW
P_{MIN} CO_2	CO_2 streams	1 bar
T_{MIN} cooling	Coolers	$T_{AMB} + \Delta T_{pp}$
$(T_{CaO,in})_{MAX}$	CaO stream	$T_{CARB} - \Delta T_{pp}$
$(T_{CaCO3,in})_{MAX}$	$CaCO_3$ stream	$T_{CARB} - \Delta T_{pp}$

Table 3
Optimization problem's independent variables with their corresponding variation range.

Independent variable	Lower bound	Upper bound
X	0.2	0.5
T_{carb}	775 °C	875 °C
P_{carb}	1.5	15
β_{MT}	1.2	14
TIT_{ST}	250 °C	650 °C
CIT_{MC}	$T_{AMB} + \Delta T_{pp}$	300 °C
$T_{CaO,in}$	310 °C	$(T_{CARB})_{MAX} - \Delta T_{pp}$
$T_{CO2,in}$	$T_{AMB} + \Delta T_{pp}$	$(T_{CARB})_{MAX} - \Delta T_{pp}$

analysis (which is only able to optimize the thermal exchange) is that the physical conditions of the streams involved in the heat transfer are continuously changed during the process, as a consequence of the turbomachinery operation optimization. The double level at the whom the optimization is executed allows to obtain a layout in which the power production maximization is reached in a complete way.

Finally, in order to prove the effectiveness of the method, random simulations are performed to observe the performance of a casual

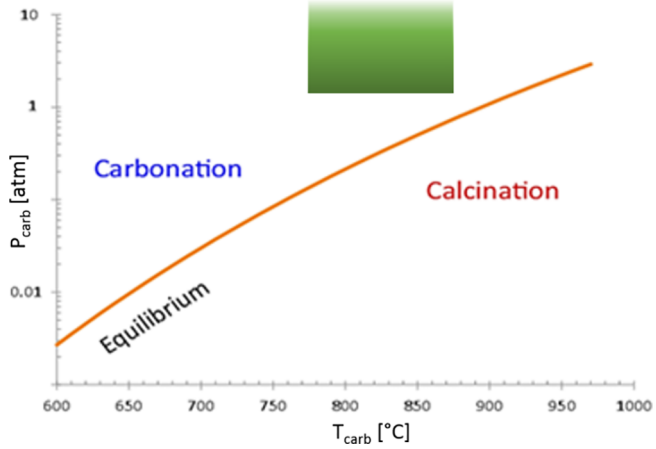

Fig. 4. Equilibrium conditions as a function of CO_2 partial pressure and temperature. The area in green represents the carbonator operating conditions investigated. (For interpretation of the references to colour in this figure legend, the reader is referred to the web version of this article.)

Table 4
Process flows conditions provided to the pinch analysis.

Stream type	Flowrate	T_{IN}	T_{OUT}
Hot	CO_2 recirculated	TOT_{MT}	CIT_{MC}
	$CaCO_3$ + CaO unreacted	T_{carb}	$T_{storage}$
Cold	CO_2 stoichiometric	$T_{storage}$	TIT_{ST}
	CaO	$T_{storage}$	$T_{CaO,in}$
	CO_2 mixed	$T_{MIX,out}$	$T_{CO2,in}$

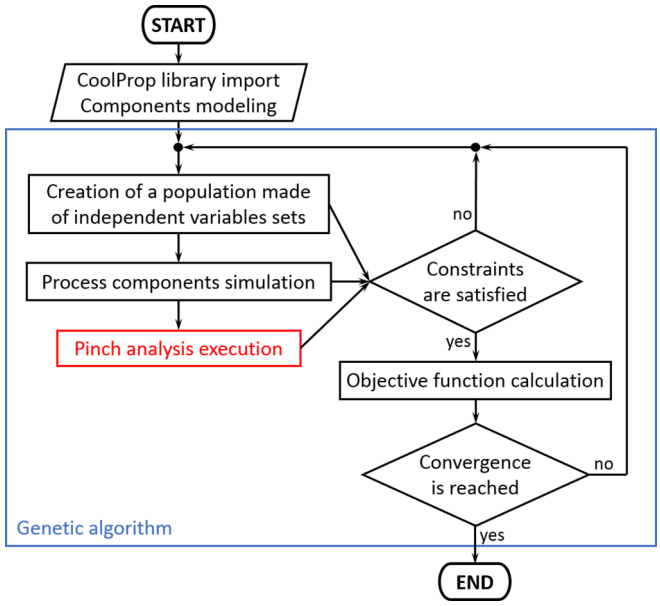

Fig. 5. Optimization structure summed up in form of flow chart: optimization of process components operation in blue, heat transfer optimization in red. (For interpretation of the references to colour in this figure legend, the reader is referred to the web version of this article.)

configuration, whose operating conditions are not optimized; Fig. 6 shows that most of the simulations have an efficiency between 3% and 13%, which is much below the optimized result reported in the following section.

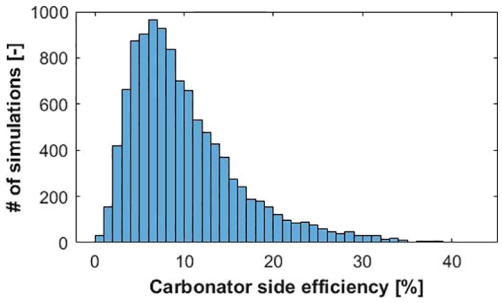

Fig. 6. Performance distribution of random simulations.

4. Results

In terms of energy performance, the carbonator side optimal operating conditions show a well-defined dependence on some of the parameters assumed as independent variables of the process. Fig. 7 shows the effect of calcium oxide activity. Evident benefits are encountered with the reduction of the inert matter participating to the process, so, for the rest of this study, the case of X = 0.5 is referred as reference case; this behavior is encountered in any layout in which the heat recovery is properly optimized, such as [15,18] and [19]. Remarkably, the CaO activity in a real plant is highly dependent on the process conditions, the particle size and the CaO precursors [8]. Any other result of the thermophysical parameters and machinery powers are given in Appendix A.

A constant trend is found for the carbonator operating temperature and for the main compressor inlet temperature: in the first case the maximum value is always reached (to maximize the main turbine production, as observed in [18;33]), while in the second case appears to be convenient to minimize this parameter in order to reduce the compression power.

The optimal carbonator pressure reaches values near to 2.8 bar, which is not a particularly demanding operating condition and is similar to the value of 3.2 bar obtained in [15] and [19]; at the same time, the main turbine pressure ratio follows closely the P_{carb} trend with the aim to keep the main compressor inlet pressure around the minimum acceptable value of 1 bar. Except for the stream composition, the main turbine operation is not very different with respect to the case in which operates the turbogas industry, which has by now reached an advanced state of development, so, implementation of suitable CO_2 turbomachinery under these operation conditions seems feasible.

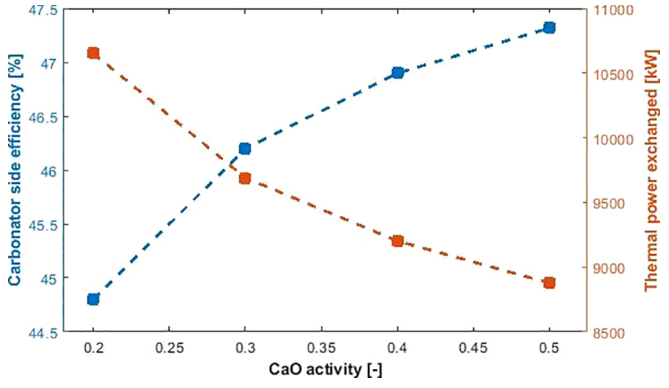

Fig. 7. Carbonator side efficiency and thermal transfer resulting from the optimization process.

Concerning the storage turbine, although reaching higher inlet temperature determines a higher power production, from the optimization results it is observed that this variable converges to relatively low values and this phenomenon can be explained as following: first, as it is well known from the exergy analysis field, it is always better to mix two flows with equal (or similar) temperatures, so, the storage turbine (ST in Fig. 2) outlet temperature tends to reach the main compressor outlet temperature. Second, heating up consistently the stoichiometric CO_2 increases the heat required from the reaction products, but, being this flowrate relatively small, the benefit encountered in the power production does not justify this substantial heat transfer. The electricity generation is therefore preferred to take place on the main turbine. Fig. 8a summarize the process components power production/absorption, while in Fig. 8b is reported the power subdivision that takes place in the plant (the term "Other losses" includes the carbonator and electric generators losses); both are for the reference case.

The power consumptions related to auxiliary cooling process are nearly negligible while the term for the solid conveying is more consistent (about one order of magnitude higher) and shows a close dependence on the calcium oxide activity. The lower is the CaO activity, the higher is the solids conveying power consumption because of the conveying of inert. In addition, the main compressor size arises to be about one half of the main turbine. Optimization results show that the CO2 mass flow rate entering the carbonator is well in excess regarding the sctechiometric amount (EI~20, an intermediate value with respect to the results in [15;19]) as can be seen in the results shown in Appendix A.

Concerning the pinch analysis, the optimization outcomes clearly demonstrate the importance of an optimal heat recovery.

As shown in Fig. 9b, pinch points are found at 725.5 °C and 123.5 °C. It is worth to notice that the pinch points are located in correspondence of the inlet temperature of two streams: the recirculated CO_2 and the mixed CO_2. This happens because the participation to the thermal transfer of these flows determines a remarkable change in the curves slope, while their distance between the pinch points is granted by the partial presence of the stoichiometric carbon dioxide, which allows the divergence above the lower pinch point and the convergence below the upper one. Another remarkable aspect is that, being the resulting turbomachinery pressure ratio and inlet/outlet temperatures very similar for the different values of CaO activity, the pinch points occurs practically at the same temperatures and, with the exception of the region above the high-temperature pinch point, the grand composite curves are nearly overlapped. Note that the grand composite curve zeroing at the highest temperature (875 °C) means only that the external heating requirement is null. For the reference case a heat exchanger network is designed in Fig. 10: hot fluids are in red, cold fluids in blue, pinch points are highlighted with dashed yellow lines, coolers are in light blue and the stream splits are named with letters form A to E; streams are abbreviated with $CaCO_3$ + CaO_{un} (solids exiting the carbonator, CO_{2REC} (CO_2 exiting the reactor), CaO (CaO reactor inlet), CO_{2MIX} (CO_2 reactor inlet), CO_{2STOIC} (CO_2 stoichiometric).

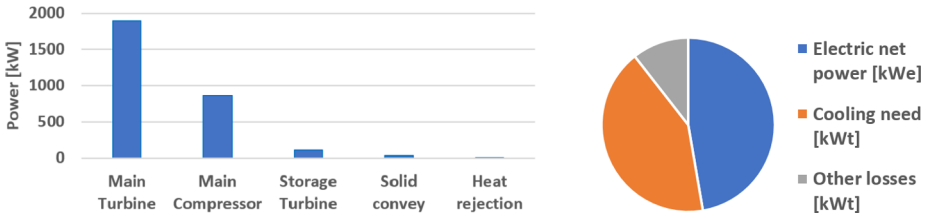

Fig. 8. a) Contributes for the electric power generation and absorption; b) Carbonator side balance of plant.

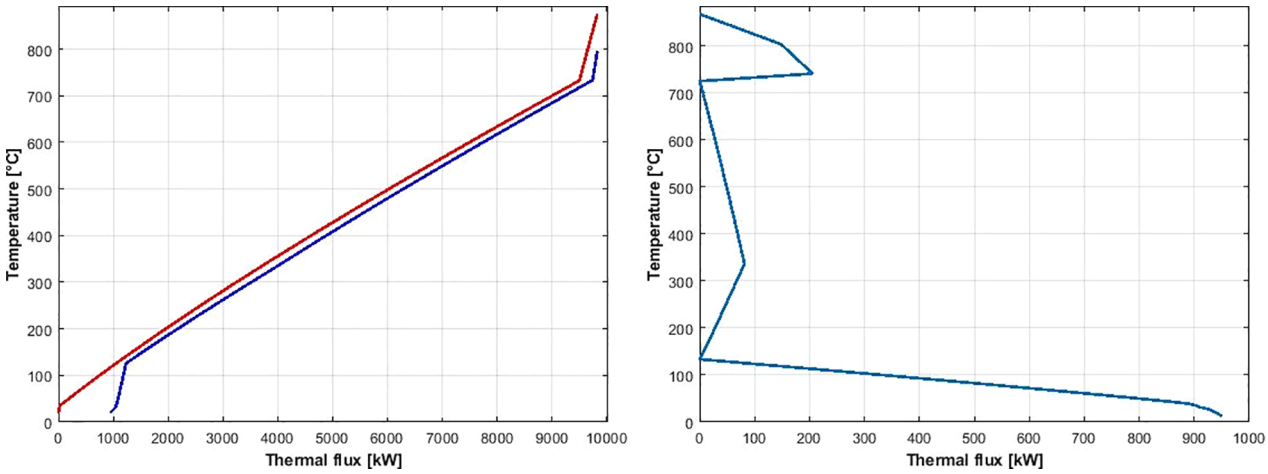

Fig. 9. a) Composite curves and b) grand composite curve for the optimized operating conditions for reference case.

The HEN layout is developed trying to follow two technical recommendations [33]: first, it is preferred to avoid solid streams split since they are more difficult to be executed if compared to fluid streams split; and second, it should be better to avoid thermal transfer between solids streams because it is based on a non-fully developed technology, so gas–gas and gas–solid heat exchange are favorite. Unluckily the configuration to the whom the genetic algorithm converges does not allow to satisfy this second recommendation because the only hot stream present above the high-temperature pinch point is the solids stream ($CaCO_3$ and unreacted CaO); anyway, a suggestion to avoid this issue is provided at the end of the present work.

Finally, it must be taken into account the possibility to eliminate the solid stream cooler below the low-temperature pinch point (colored with striped light blue in Fig. 10) and directly send the flow to its storage; a little improvement is obtained in this way because both the use of a heat exchanger and the parasitic electric consumption for heat rejection are avoided and this shouldn't constitute a critical issue for the $CaCO_3$ storage since the stream is at relatively low temperature.

5. Multi-objective optimization

As observed from the pinch analysis results and HEN (Figs. 7 and 8), the optimization process seems to converge to configurations that enhance the heat exchange stage, making the hot and cold composite curves to approach each other as much as possible. Anyway, despite this phenomenon brings benefits to the plant efficiency, the resulting HEN may show some criticalities both in terms of complexity and dimensions (heat transfer area). As an attempt to overcome this issue it is introduced a new parameter which should act as an indicator of the heat recovery system stiffness: the UA_{eq} (equivalent product between the global heat transfer coefficient and the exchange area) calculated on the discretized hot and cold composite curves (Eq. (4)) without taking into account the external cooling step, since this process doesn't constitute a criticality for the heat exchanger network. Assuming the equivalent product between U and A instead of only the equivalent A allows to avoid taking into account the different effectiveness characterizing the heat exchange in case of gas–gas, gas–solid or solid–solid thermal transfer and therefore makes unnecessary to address a coherent value of U for any stream coupling. The total UA of the real HEN will be higher than the value found with this indicator since it's obtained pretending that all the hot and cold fluids are mixed together and only the two resulting flows participate to the heat transfer, which is an ideal condition. Anyway, as already explained, this parameter provides only a qualitative and not quantitative information for the purposes of this analysis. There can be two causes for an increase of the equivalent UA: one consists in an increase of the power transferred between the streams, while the other is represented by the approach of the two composite curves; both of them determine a growth of the HEN size, but the last one may bring to an additional issue, which is the formation of pinch points. This fact, according to the pinch analysis theory, leads to the conceptual separation of the heat recovery process into two (or more) subsystems which are energy independent between them and don't share any heat exchanger; as a consequence, the number of units used for the thermal transfer becomes higher and the HEN complexity tends to increase.

$$UA_{eq} = \sum_i \left[\frac{\phi_i}{\Delta T_{lm,i}} \right] \tag{4}$$

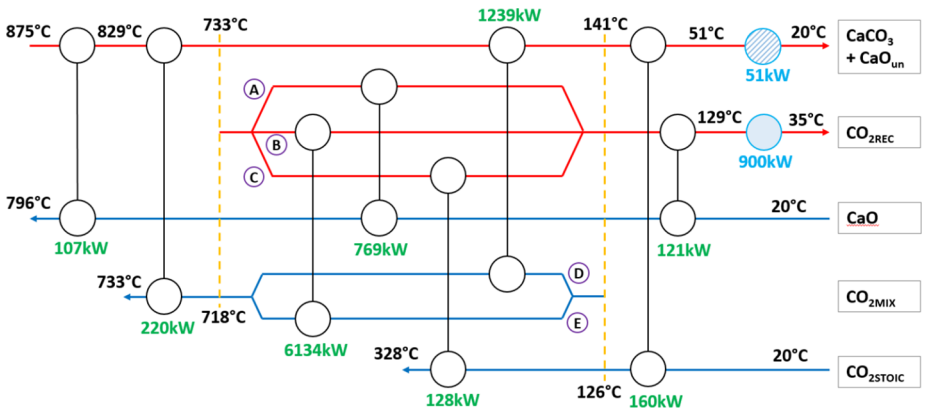

Fig. 10. Heat exchanger network for the optimized operating condition for reference case.

where ϕ_i is the thermal flux and $\Delta T_{lm,i}$ stands for the logarithmic mean temperature difference, both defined for the i-interval.

Finally, in addition to the aspects already explained, the use of UA_{eq} as second objective function instead of the plant cost (which would allow to perform an economic analysis) is due to the fact that some of the main components involved in the process are still in an early stage of development, so representative data are not available yet.

At this point is possible to setup a double-target optimization whose objective functions are the carbonator side efficiency (η_{carb}) and the UA_{eq}; the entire plant simulation remains unchanged with respect to the investigation previously performed. Results show clearly the effects of an optimal thermal transfer process on the plant performance: the more effective is the heat transfer between reactants and products, the higher are both the efficiency and the equivalent UA. As expected, for the same carbonator side efficiency value, lower values of calcium oxide reactivity determine an increase in the HEN dimensions because of the higher amount of inert matter that takes part to the process.

In Fig. 11a are reported the pareto curves for the multi-objective optimization, while 11b shows the values reached by the independent variables normalized by their corresponding variation range for the reference case; the main compressor inlet temperature is the only term to present a constant behavior since it stays practically always at its lower bound, while the other parameters have different trends. In particular, the carbonator pressure and the main turbine pressure ratio are very strictly bonded between them, confirming the convenience to reach a main turbine outlet pressure close to 1 bar (set as the minimum achievable value); higher values of both contribute to simplify the thermal transfer system. The same effect is obtained with lower carbonator temperatures and lower reactor inlet temperatures. This is due to the fact that all these trends determine a decrease of the temperatures of both the reactants that must be heated up and the products that needs to be cooled down; as a consequence, accepting an efficiency reduction (which can be not particularly disadvantageous, especially when its value is high) it is possible to consistently reduce the HEN size and perhaps even its complexity (although this must be demonstrated).

From the previous analysis and with the aim to observe the possible HEN topology changes, several heat exchangers networks are proposed for different values of the equivalent UA. The cases considered are chosen in reference to the configuration that provides the higher UA_{eq} value (which coincides with the single objective optimization result) with a CaO activity set to the reference value. Fig. 12 shows the resulting grand composite curves for these selected configurations.

As expected, the thermal flux exchanged between the fluids decreases with the reduction of the equivalent UA; the hot and cold composite curves tend any way to approach each other, but with a lowering effectiveness. This effect is shown in Fig. 8: the two pinch points present in the first configuration gradually disappear when the UA_{eq} becomes smaller, while the cooling need increases as a consequence of the efficiency reduction. This means that the thermal transfer is not executed in the best way since the same heat exchange could be performed with a higher value of the minimum temperature difference achievable (in particular, 22 °C for the case of 40%UA_{max} and 58 °C for 10% UA_{max}); however, this does not represent a problem because avoiding these pinch points is exactly one of the purposes of this investigation.

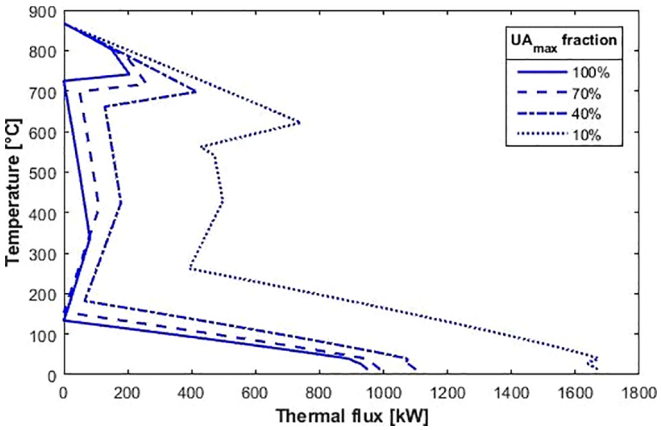

Fig. 12. Grand composite curve for the investigated cases (X = 0.5).

The layouts reported in Appendix B are designed with the same criteria explained in the previous optimization. From these layouts it is possible to observe that the heat exchanger arrangement does not undergo radical changes, since the stream splits differ only in the percentage amounts but not in their position or number. Furthermore, regarding their size and complexity, performing a worst heat recovery allows to reduce the heat exchangers dimensions and, in some cases, their number, obtaining therefore a simpler network. Finally, it should not be forgotten that the solid stream cooling ($CaCO_3$ and unreacted CaO) can be theoretically avoided sending it directly to its storage, so it is possible to imagine one of the two coolers as absent.

6. System optimization improvement

In order to refine from a technological perspective the results achieved from the energy optimization, as avoiding the solid–solid heat exchange, a single-objective optimization with an additional constraint (Eq. (5)) is performed. This equation imposes an upper limit for the temperature of the CaO entering the carbonator ($T_{CaO,in}$); in this way this cold stream does not appear above the high-temperature pinch point where the only hot flow is the solid stream exiting the carbonator.

$$T_{CaO,in} \leq TOT_{MT} - \Delta T_{pp} \tag{5}$$

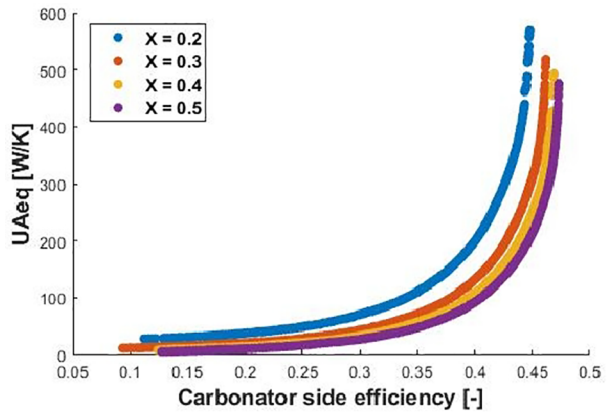

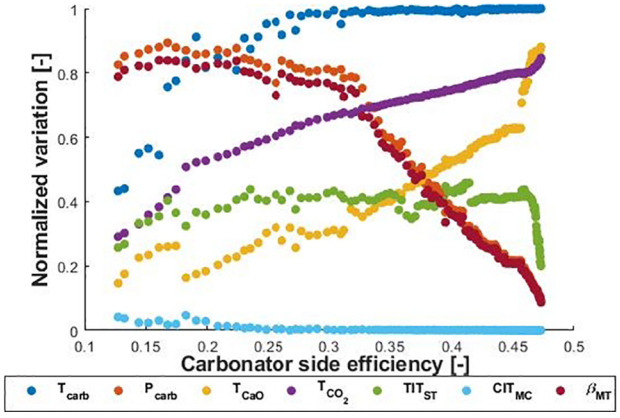

Fig. 11. a) Pareto curves from the multi-objective optimization and b) variables normalized trend along the pareto for reference case.

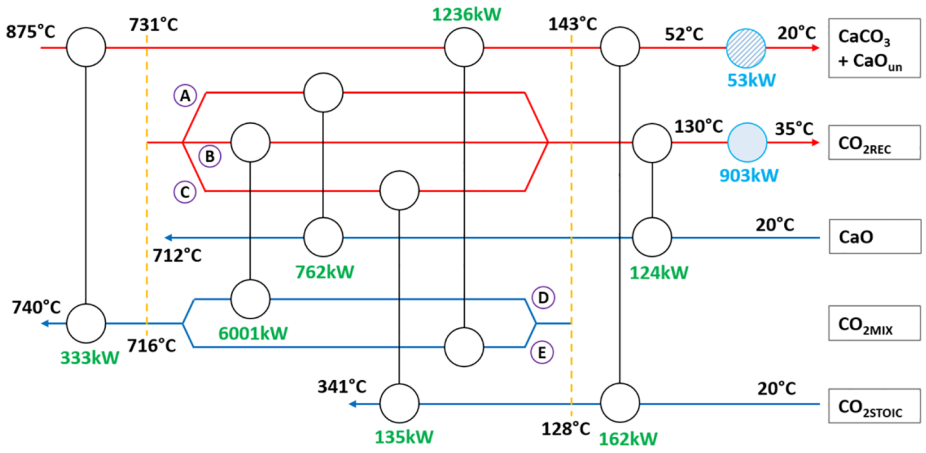

Fig. 13. Heat exchanger network for the optimal operating conditions (in reference case), which avoid solid–solid transfer.

Fig. 13 shows the designed HEN considering the previous constrain for the reference case. As consequence of this new design, the plant is not only it's managed to overcome the problem of solid–solid thermal transfer, but the number of heat exchangers is decreased by one. Another positive aspect is that the carbonator side efficiency decrease is practically negligible since in relative terms is equal to 0.16%. Furthermore, the other elements disposition remains equal to the original case and the total UA undergoes only a little decrease (3.4% in relative terms). These last aspects demonstrate the high complexity and flexibility of the objective function, since even much different values assumed by the independent variables can bring to results very close to the optimum.

As shown in Fig. 14, the optimum carbonator side consist of eight HEXs, of which: two are gas–gas heat exchangers, five are gas–solid heat exchangers and one is a cooler.

As demonstrated by the results obtained from the energy optimizations performed up to this point, the formation of a high-temperature pinch point occurs whenever the total CO_2 entering the carbonator has a temperature higher than the main turbine outlet temperature. So, looking at the advantages obtained from the last analysis, another attempt to find a simpler design for the thermal recovery process is performed with the addition of another constraint (Eq. (6)) similar to previous one, but applied to the other carbonator inlet stream: the mixed carbon dioxide.

$$T_{CO_2,in} \leq TOT_{MT} - \Delta T_{pp} \tag{6}$$

However, as shown in Fig. 15, the effects encountered with this additional limitation are more complex than the previous ones. In fact, despite both the pinch points disappear and the number of heat exchangers decreases to five, the carbonator side efficiency reduction (6.8% in relative terms) and the total UA increase (9.8% in relative terms) constitute two considerable drawbacks. The reason of that is due to the fact that the mixed CO_2 is one of the most important contributors to the heat recovery and a restriction on this parameter will generate a much more consistent penalty with respect to the one applied on the $CaCO_3$ stream.

The convenience of this layout should be therefore evaluated for what this configuration actually represents: a compromise between good performances and a simple HEN structure, obtained at the price of a consistent size of the heat recovery system.

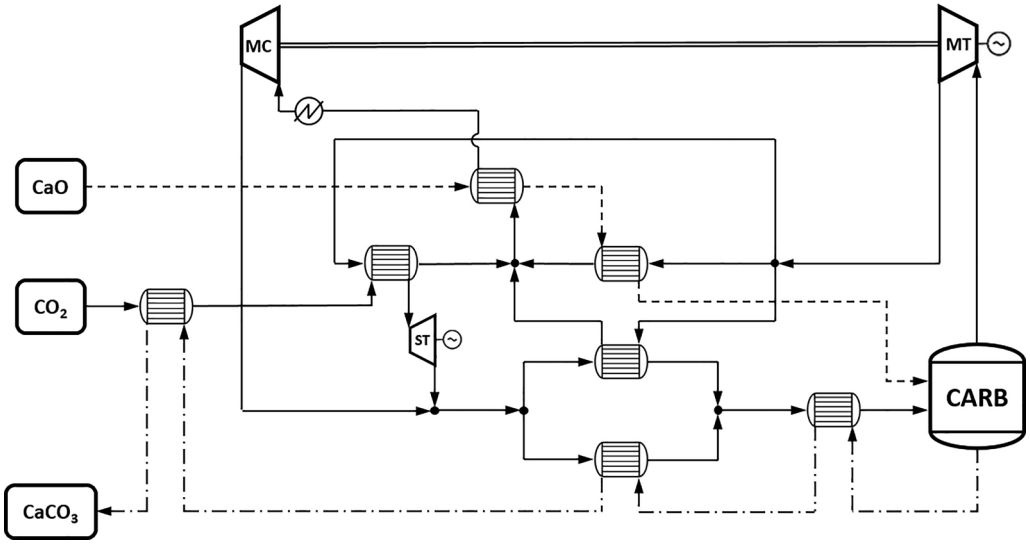

Fig. 14. Process integration scheme from the HEN analysis shown in Fig. 9.

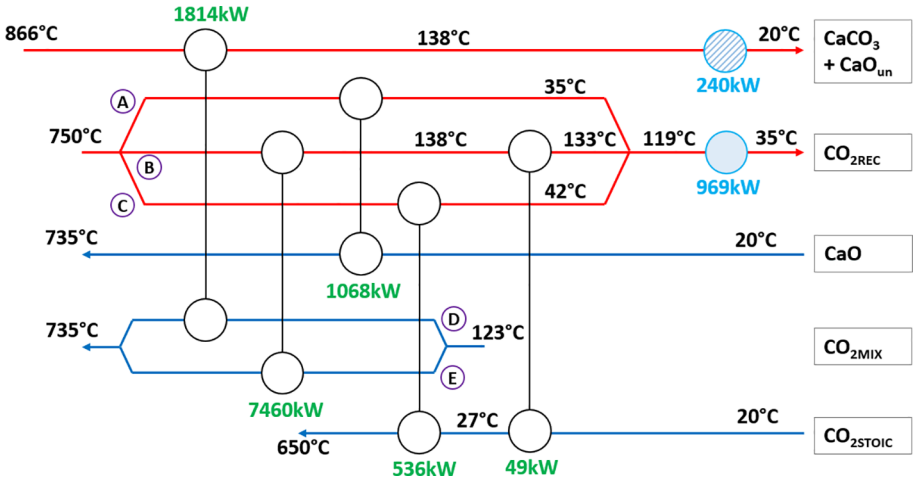

Fig. 15. Heat exchanger network for the optimized conditions with double carbonator inlet temperature constrain for the reference case.

7. General comments

This section is devoted to some considerations obtained in the present work but with a more general extent and therefore possibly useful in other fields. One aspect characterizing the HEATSEP that may represent a limitation to this kind of analysis is that the HEN is obtained in the postprocessing phase and therefore it is not possible to make considerations or changes during the optimization process, fact that becomes important in presence of multiple pinch points. However, this drawback can be limited looking at the trend showed in a first optimization run, understanding the tendencies that characterize the process and introducing suitable changes in a second run, making a kind of retrofit. In this way is obtained a more favorable configuration which met multiple criteria and preferences.

Another noticeable aspect is that, for problems with a sufficient number of independent variables, it is no wonder that a relatively consistent change or limitation to some process inputs lead to optimized configurations with still good performances. In fact, the method presents a non-negligible flexibility in the optimum search, since a worsening in the thermal transfer phase can be partially compensated by a change occurring in the components operating conditions and vice versa.

Finally, it is interesting to notice that some parameters/variables have only a partial effect on the optimization process. For example, the CaO conversion has important effects on the carbonator side efficiency, but it only affects the heat transfer process. The process components operating conditions are not influenced by this parameter, so the CO_2 excess index, the carbonator temperature, the turbomachinery pressure ratios and their powers remain practically unchanged, as reported in Appendix A.

8. Conclusions

The direct integration of a Calcium-Looping in a small/medium central tower CSP plant is analyzed in the present work. The aim of the study is to perform an energy optimization of the carbonation side, where occurs the energy discharge process, and to execute it without the limitation of assume a certain heat exchanger network; it is therefore chosen a suitable method in which the process components and the heat transfer are simultaneously optimized.

The results obtained show the convenience in reaching high values of CaO reactivity (X = 0.5) and higher carbonator operating temperature (875 °C), while lower main compressor inlet temperatures must be preferred (35 °C); intermediate and non-demanding pressures are reached for the carbonator functioning (2.8 bar). Furthermore, the algorithm converges to configurations in which the heat recovery between reactants and products is performed in a very effective way, such that high temperatures of the two carbonator inlet streams are achieved; however, this leads to relatively complex heat exchanger networks. The multi-objective optimization demonstrates the possibility to reach smaller and simpler thermal recovery systems at the price of an efficiency reduction, providing a criterion for the choice of a compromise between these two fundamental aspects of the plant. Considering the number of independent variables assumed and the double level (heat exchange and components operation) at the whom the optimization is performed, it is possible to state that the results obtained represent in absolute terms the highest achievable carbonator side efficiency for the configuration assumed and demonstrate what are the key features characterizing this plant portion, providing a direction to the whom future researches may focus. Finally, with the insertion of a further constraint, the issue of solid–solid heat transfer is overcome in the last part of the work and an additional suggestion for the HEN simplification is provided at the end of the study.

Declaration of Competing Interest

The authors declare that they have no known competing financial interests or personal relationships that could have appeared to influence the work reported in this paper.

Acknowledgement

This work has been founded and conducted within the European Project SOCRATCES (SOlar Calcium-looping integRAtion for Thermo-Chemical Energy Storage) GA 727348.

Appendix A. Single-objective optimization: Thermophysical results

	X = 0.2	X = 0.3	X = 0.4	X = 0.5
EI [−]	19.9	20.1	20.1	20.1
β_{MT} [−]	2.65	2.65	2.66	2.67
β_{MC} [−]	2.94	2.94	2.95	2.96
Cooling need [kW_t]	976	962	955	951
	X = 0.2	X = 0.3	X = 0.4	X = 0.5
MT [kW]	1895	1895	1896	1896
MC [kW]	864	864	865	865
ST [kW]	114.5	113.1	112.4	111.8
Solid convey [kW_e]	77.7	53.2	41.1	33.9
Heat rejection [kW_e]	7.81	7.70	7.64	7.60
Total net power [kW_e]	1026	1049	1060	1067
Carbonator side efficiency [%]	44.80	46.20	46.90	47.32

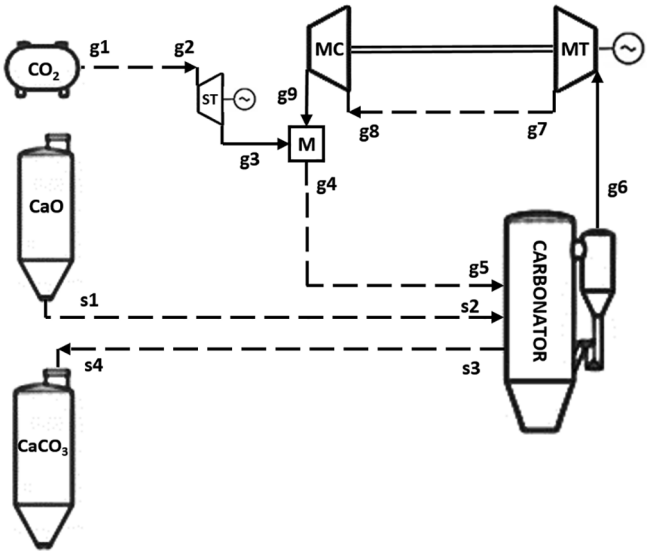

	X = 0.2			X = 0.3			X = 0.4			X = 0.5		
	P [bar]	T [°C]	$\dot{m}$[kg/s]	P [bar]	T [°C]	$\dot{m}$[kg/s]	P [bar]	T [°C]	$\dot{m}$[kg/s]	P [bar]	T [°C]	$\dot{m}$[kg/s]
g1	75	20	0.566	75	20	0.561	75	20	0.559	75	20	0.557
g2	74.25	332	0.566	74.25	30	0.561	74.25	329	0.559	74.25	328	0.557
g3	2.93	118	0.566	2.94	116	0.561	2.95	116	0.559	2.96	116	0.557
g4	2.93	125	11.3	2.94	125	11.3	2.95	125	11.2	2.96	126	11.2
g5	2.76	751	11.3	2.76	742	11.3	2.77	737	11.2	2.79	733	11.2
g6	2.76	875	10.7	2.76	875	10.7	2.77	875	10.7	2.79	875	10.6
g7	1.04	734	10.7	1.04	734	10.7	1.04	733	10.7	1.04	732	10.6
g8	1	35	10.7	1	35	10.7	1	35	10.7	1	35	10.6
g9	2.93	126	10.7	2.94	126	10.7	2.95	126	10.7	2.96	126	10.6
s1	1	20	3.60	1	20	2.38	1	20	1.78	1	20	1.42
s2	1	771	3.60	1	775	2.38	1	787	1.78	1	796	1.42
s3	1	875	4.17	1	875	2.94	1	875	2.34	1	875	1.98
s4	1	20	4.17	1	20	2.94	1	20	2.34	1	20	1.98

Appendix B. Multi-objective optimization: Pinch analysis results

$UA_{eq,max}$ fractions	η_{carb}	Flow fractions				
		A	B	C	D	E
100%	47.32%	10.9%	87.2%	1.8%	16.8%	83.2%
70%	46.79%	13.0%	84.0%	3.0%	19.8%	80.2%
40%	44.41%	16.3%	78.4%	5.3%	24.1%	75.9%
10%	34.97%	25.2%	50.1%	24.7%	36.9%	63.1%

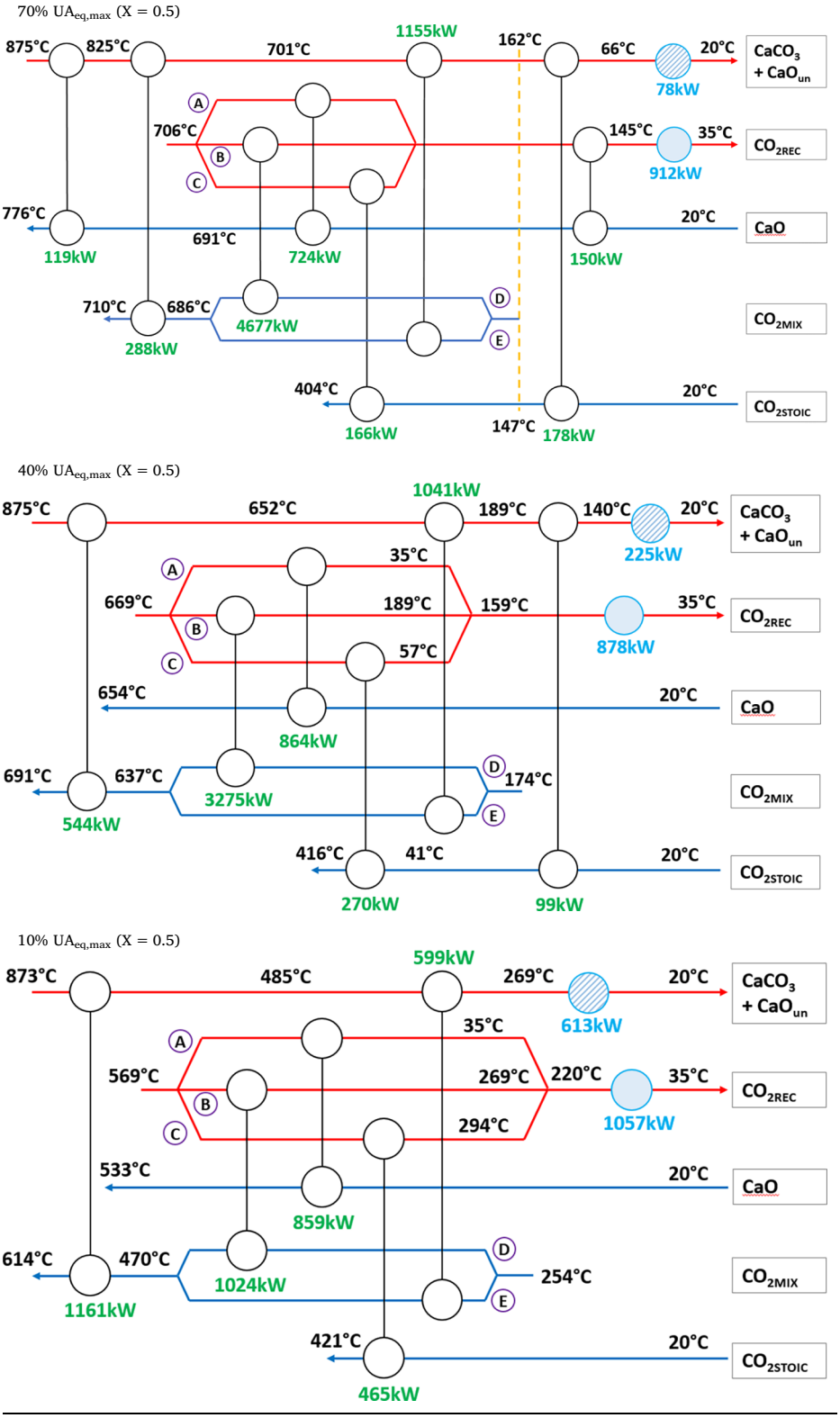
70% UA$_{eq,max}$ (X = 0.5)
875°C
825°C
701°C
1155kW
162°C
66°C
20°C
78kW
CaCO$_3$ + CaO$_{un}$
A
706°C
B
C
145°C
35°C
912kW
CO$_{2REC}$
776°C
691°C
20°C
CaO
119kW
724kW
150kW
710°C
686°C
4677kW
D
E
288kW
CO$_{2MIX}$
404°C
20°C
CO$_{2STOIC}$
166kW
147°C
178kW
40% UA$_{eq,max}$ (X = 0.5)
875°C
652°C
1041kW
189°C
140°C
20°C
225kW
CaCO$_3$ + CaO$_{un}$
35°C
A
669°C
189°C
159°C
35°C
B
878kW
CO$_{2REC}$
C
57°C
654°C
20°C
CaO
864kW
691°C
637°C
D
174°C
3275kW
CO$_{2MIX}$
544kW
E
416°C
41°C
20°C
CO$_{2STOIC}$
270kW
99kW
10% UA$_{eq,max}$ (X = 0.5)
873°C
485°C
599kW
269°C
20°C
613kW
CaCO$_3$ + CaO$_{un}$
35°C
A
569°C
269°C
220°C
35°C
B
CO$_{2REC}$
C
294°C
1057kW
533°C
20°C
CaO
859kW
614°C
470°C
D
254°C
1024kW
CO$_{2MIX}$
1161kW
E
421°C
20°C
CO$_{2STOIC}$
465kW

References

[1] Tasbirul Islam M, Huda N, Abdullah A, Saidur R. A comprehensive review of state-of-the-art concentrating solar power (CSP) technologies: current status and research trends. Renew Sustain Energy Rev 2018;91:987–1018.
[2] SunShot Initiative – Solar Energy Technologies Office - U.S. Department of Energy, Tackling Challenges In Solar: 2014 Portfolio, 2014.
[3] European Solar Thermal Electricity Association, "Solar Thermal Electricity Strategic research agenda 2020-2025", Dec. 2012.
[4] Kuravi S, Trahan J, Goswami D, Rahman M, Stefanakos E. Thermal energy storage technologies and systems for concentrating solar power plants. Prog Energy Combust Sci 2013;39:285–319.
[5] Sunku Prasad J, Muthukumar P, Desai F, Basu DN, Rahman M. A critical review of high-temperature reversible thermochemical energy storage systems. Appl Energy 2019;254:113733.
[6] Chen X, Zhang Z, Qi C, Ling X, Peng H. State of the art on the high-temperature thermochemical energy storage systems. Energy Convers Manage 2018;177:792–815.
[7] Ervin G. Solar heat storage using chemical reactions. J Solid State Chem 1977;22:51–61.
[8] Ortiz C, Valverde J, Chacartegui R, Perez-Maqueda L, Giménez P. The calcium-looping (CaCO3/CaO) process for thermochemical energy storage in concentrating solar power plants. Renew Sustain Energy Rev 2019;113.
[9] Bioazul, "Deliverable D8.1 - First Innovation Evaluation report", 2018.
[10] Pardo P, Deydier A, Anxionnaz-Minvielle Z, Rougé S, Cabassud M, Cognet P. A review on high temperature thermochemical heat energy storage. Renew Sustain Energy Rev 2014;32:591–610.
[11] "Socratces Project | Energy Storage Technologies Viable & Sustainable", [Online]. Available: https://socratces.eu/. [accessed 07.19].
[12] Stein W, Buck R. Advanced power cycles for concentrated solar power. Sol Energy 2017;152:91–105.
[13] Kolios A, Paganini S, Proia S. Development of thermodynamic cycles for concentrated solar power plants. Int J Sustain Energy 2013;32:296–314.
[14] Dunham M, Iverson B. High-efficiency thermodynamic power cycles for concentrated solar power systems. All Faculty Publications 2014;30:758–70.
[15] Chacartegui R, Alovisio A, Ortiz C, Valverde J, Verda V, Becerra J. Thermochemical energy storage of concentrated solar power by integration of the calcium looping process and a CO2 power cycle. Appl Energy 2016;173:589–605.
[16] Edwards S, Materić V. Calcium looping in solar power generation plants. Sol Energy 2012;86:2494–503.
[17] Xiaoyi C, Dong Z, Yan W, Xiang L, Xiaogang J. The role of sensible heat in a concentrated solar power plant with thermochemical energy storage. Energy Convers Manage 2019;190:42–53.
[18] Ortiz C, Chacartegui R, Valverde J, Alovisio A, Becerra J. Power cycles integration in concentrated solar power plants with energy storage based on calcium looping. Energy Convers Manage 2017;149:815–29.
[19] Ortiz C, Romano M, Valverde J, Binotti M, Chacartegui R. Process integration of calcium-looping thermochemical energy storage system in concentrating solar power plants. Energy 2018;155:535–51.
[20] Karasavvas E, Panopoulos K, Papadopoulou S, Voutetakis S. Design of an integrated CSP-calcium looping for uninterrupted power production through energy storage. Chem Eng Trans 2018;70:2131–6.
[21] Fernandex R, Ortiz C, Chatartegui R, Valverde e J, Becerra J. Dispatchability of solar photovoltaics from thermochemical energy storage. Energy Convers Manage 2019;191:237–46.
[22] Kemp I. Pinch Analysis and Process Integration. Butterworth-Heinemann; 2007.
[23] Lazzaretto A, Toffolo A. A method to separate the problem of heat transfer interactions in the synthesis of thermal systems. Energy 2008;33:163–70.
[24] Valverde J, Medina S. Crystallographic transformation of limestone during calcination under CO2. PCCP 2015;34:21912–26.
[25] Berger E. Effect of steam on the decomposition of limestone. Ind Eng Chem 1927;19:594–6.
[26] Valverde J, Medina S. Reduction of calcination temperature in the calcium looping process for CO2 capture by using helium. In situ XRD analysis. ACS Sustain Chem Eng 2016;4:7090–7.
[27] Ortiz C, Valverde J, Chacartegui R, Perez-Maqueda L. Carbonation of limestone derived CaO for thermochemical energy storage: from kinetics to process integration in concentrating solar plants. ACS Sustainable Chem Eng 2018;6:6404–17.
[28] Zhao M, Minett A, Harris A. A review of techno-economic models for the retrofitting of conventional pulverised-coal power plants for post-combustion capture (PCC) of CO2. Energy Environ Sci 2013;6:25–40.
[29] European Commission, "Carbon capture by means of indirectly heated carbonate looping process", vol. 9424, 2014.
[30] Hilz J, Helbig M, Haaf M, Daikeler A, Ströhle J, Epple B. Long-term pilot testing of the carbonate looping process in 1 MWth scale. Fuel 2017;210:892–9.
[31] U.S. Department of Energy, "Falling Particles: Concept Definition and Capital Cost Estimate", 2016.
[32] Arias B, Abanades J, Grasa G. An analysis of the effect of carbonation conditions on CaO deactivation curves. Chem Eng J 2011;167:255–61.
[33] Alovisio A, Chacartegui R, Ortiz C, Valverde J, Verda V. Optimizing the CSP-calcium looping integration for thermochemical energy storage. Energy Convers Manage 2017;136:85–98.
[34] Toffolo A. A synthesis/design optimization algorithm for Rankine cycle based energy systems. Energy 2014;66:115–27.
[35] Toffolo A, Lazzaretto A, Morandin M. The HEATSEP method for the synthesis of thermal systems: an application to the S-Graz cycle. Energy 2010;35:976–81.
[36] Mesfun S, Toffolo A. Optimization of process integration in a Kraft pulp and paper mill – Evaporation train and CHP system. Appl Energy 2013;107:98–110.
[37] A. Alovisio, "Process Integration Of A Thermochemical Energy Storage System Based On Calcium Looping Incorporating Air/CO2 Cycles In CSP Power Plants", 2015.
[38] Chase M. NIST-JANAF themochemical tables, Fourth edition. J Phys Chem Ref Data 1998.
[39] I. Bell, J. Wronski, S. Quoilin and V. Lemort, "Welcome to CoolProp — CoolProp 6.3.0 documentation", [Online]. Available: http://www.coolprop.org/. [accessed 2019].